

Electron transport in polycyclic hydrocarbon molecules: A study of shot noise contribution to the power spectrum

Santanu K. Maiti^{1,2,*}

¹*Theoretical Condensed Matter Physics Division, Saha Institute of Nuclear Physics,
1/AF, Bidhannagar, Kolkata-700 064, India*

²*Department of Physics, Narasinha Dutt College, 129, Belilious Road, Howrah-711 101, India*

Abstract

We study electron transport in polycyclic hydrocarbon molecules attached to two semi-infinite one-dimensional metallic electrodes by the use of Green's function formalism. Parametric calculations based on the tight-binding framework are given to investigate the transport properties through such molecular bridges. In this context we also discuss noise power of current fluctuations and focus our attention on the shot noise contribution to the power spectrum. The electron transport properties are significantly influenced by (a) length of the molecule, (b) molecule-electrode interface geometry and (c) molecular coupling strength to the electrodes.

PACS No.: 73.23.-b; 73.63.Rt; 73.40.Jn; 81.07.Nb

Keywords: Polycyclic hydrocarbon molecules; Interference effect; Conductance; I - V characteristic; Shot noise.

***Corresponding Author:** Santanu K. Maiti
Electronic mail: santanu.maiti@saha.ac.in

1 Introduction

The advancements in nanoscience and technologies prompting a growing number of researchers across multiple disciplines to attempt to devise innovative ways for decreasing the size and increasing the performance of microelectronic circuits. One possible route is based on the idea of using molecules and molecular structures as functional devices. During 1970's Avriam *et al.* [1] first studied theoretically the electron transport through molecular bridge systems. Later several numerous experiments [2, 3, 4, 5, 6] have been carried out on electron transport through molecules placed between two non-superconducting electrodes with few nanometer separation. Though in literature both theoretical [7, 8, 9, 10, 11, 12] as well as experimental [2, 3, 4, 5, 6] works on electron transport in several bridge systems are available, yet lot of controversies are still present between the theory and experiment, and the complete knowledge of the conduction mechanism in this scale is not very well established even today. Molecular transport properties are characterized by several important factors. First one, of course, is the quantization of energy levels associated with the identity of the molecule itself and the quantum interference of electron waves [13, 14, 15, 16, 17, 18, 19] associated with the geometry that the molecule adopts within the junction. Second are the different parameters of the Hamiltonian that describe the molecular system, the electronic structure of the molecule and the molecular coupling to the side attached electrodes. To design molecular electronic devices with specific properties, it is important to study structure-conductance relationships and in a very recent work Ernzerhof *et al.* [20] have presented a general design principle and performed several model calculations to demonstrate the concept. The knowledge of current fluctuations (of thermal or quantum origin) also gives many key ideas for fabrication of efficient molecular devices. Blanter *et al.* [21] have described elaborately how the lowest possible noise power of the current fluctuations can be determined in a two-terminal conductor. The steady state current fluctuations, the so-called shot noise, is a consequence of the quantization of charge and it can be used to obtain information on a system which is not directly available through conductance measurements. The noise power of current fluctuations provides an additional important information about the electron correlation by calculating the Fano factor (F) which directly informs us whether the mag-

nitude of the shot noise achieves the Poisson limit ($F = 1$) or the sub-Poisson ($F < 1$) limit.

There exist different *ab initio* methods for the calculation of conductance [22, 23, 24, 25, 26, 27, 28] through a molecular bridge. At the same time the tight-binding model has been extensively studied in the literature and it has also been extended to DFT transport calculations [29]. The study of static density functional theory (DFT) [30] within the local-density approximation (LDA) to investigate the electronic transport through nanoscale conductors, like atomic-scale point contacts, has met with nice success. But, when this similar theory applies to molecular junctions, theoretical conductances achieve larger values compared to the experimental predictions and these quantitative discrepancies need extensive study in this particular field. In a recent work, Sai *et al.* [31] have predicted a correction to the conductance using the time-dependent current-density functional theory since the dynamical effects give significant contribution in the electron transport, and illustrated some important results with specific examples. Similar dynamical effects have also been reported in some other recent papers [32, 33], where authors have abandoned the infinite reservoirs, as originally introduced by Landauer, and considered two large but finite oppositely charged electrodes connected by a nanojunction. Our aim of the present paper is to reproduce an analytic approach based on the tight-binding model to characterize the electronic transport properties through some polycyclic hydrocarbon molecules and focus our attention on the effects of (a) length of the molecules, (b) molecule-to-electrode coupling strength and (c) quantum interferences of electronic waves passing through different arms of the molecular rings. We utilize a simple parametric approach [34, 35, 36, 37, 38, 39] for these calculations. The model calculations are motivated by the fact that the *ab initio* theories are computationally too expensive, while the model calculations by using the tight-binding framework are computationally very cheap and also provide a worth insight to the problem. In our present study attention is drawn on the qualitative behavior of the physical quantities rather than the quantitative ones. Not only that, the *ab initio* theories do not give any new qualitative behavior for this particular study in which we concentrate ourselves.

We organize the paper specifically as follows. Section 2 describes very briefly the methodology for the calculation of the transmission probability (T), current (I) and noise power of current fluctuations (S)

through a molecule sandwiched between two metallic electrodes by using the Green's function formalism. In Section 3, we study the behavior of the conductance as a function of the injecting electron energy, current and noise power of its fluctuations as a function of the applied bias voltage for the different polycyclic hydrocarbon molecules (Fig. 1). Finally, we summarize our results in Section 4.

2 Theoretical formulation

In this section we briefly describe the technique for the calculation of transmission probability (T), conductance (g), current (I) and noise power of its fluctuations (S) through a molecule (schematically represented as in Fig. 1) attached to two semi-infinite one-dimensional (1D) metallic electrodes by using the Green's function approach.

At low voltage and low temperature, the conductance g of the molecule is given by the Landauer conductance formula [40],

$$g = \frac{2e^2}{h} T \quad (1)$$

where the transmission probability T is written in the form [40],

$$T = \text{Tr} [\Gamma_S G_M^r \Gamma_D G_M^a] \quad (2)$$

where G_M^r (G_M^a) is the retarded (advanced) Green's function of the molecule and Γ_S (Γ_D) describes its coupling to the source (drain). The effective Green's function of the molecule is expressed as,

$$G_M = (E - H_M - \Sigma_S - \Sigma_D)^{-1} \quad (3)$$

where E is the energy of the source electron and H_M is the Hamiltonian of the molecule which can be written in the tight-binding model within the non-interacting picture like,

$$H_M = \sum_i \epsilon_i c_i^\dagger c_i + \sum_{\langle ij \rangle} t (c_i^\dagger c_j + c_j^\dagger c_i) \quad (4)$$

Here, ϵ_i 's are the site energies and t is the nearest-neighbor hopping integral. In Eq.(3), Σ_S and Σ_D correspond to the self-energies due to coupling of the molecule to the two electrodes. Now all the information about the molecule-to-electrode coupling are included into these two self-energies and are described through the use of Newns-Anderson chemisorption theory [34, 35].

The current passing through the molecule can be considered as a single electron scattering process

between the two reservoirs of charge carriers. The current-voltage relation can be obtained from the expression [40],

$$I(V) = \frac{e}{\pi\hbar} \int_{-\infty}^{\infty} (f_S - f_D) T(E) dE \quad (5)$$

where the Fermi distribution function $f_{S(D)} = f(E - \mu_{S(D)})$ with the electrochemical potentials $\mu_{S(D)} = E_F \pm eV/2$. For the sake of simplicity, here we assume that the entire voltage is dropped

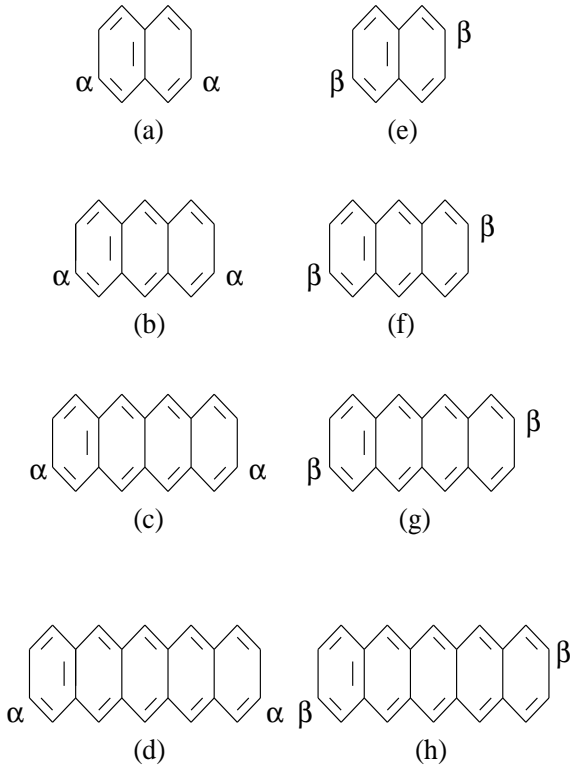


Figure 1: Schematic view of four polycyclic hydrocarbon molecules those are attached to two electrodes, namely, source and drain, in *cis* (α - α) and *trans* (β - β) configurations by thiol (sulfur-hydrogen i.e., S-H bond) groups. These four molecules are defined as: naphthalene (two rings), anthracene (three rings), tetracene (four rings) and pentacene (five rings).

across the conductor-electrode interfaces and this assumption does not significantly affect the qualitative aspects of the I - V characteristics. The assumption is based on the fact that the electric field inside the molecule, especially for short molecules, seems to have a minimal effect on the conductance-voltage characteristics. On the other hand, for quite

larger molecules and high bias voltage, the electric field inside the molecule may play a more significant role depending on the internal structure of the molecule [41], though the effect is too small.

The noise power of the current fluctuations is calculated from the relation [21],

$$S = \frac{2e^2}{\pi\hbar} \int_{-\infty}^{\infty} [T(E) \{f_S(1-f_S) + f_D(1-f_D)\} + T(E) \{1-T(E)\} (f_S - f_D)^2] dE \quad (6)$$

where the first two terms of this equation correspond to the equilibrium noise contribution and the last term gives the non-equilibrium or shot noise contribution to the power spectrum. By calculating the noise power of the current fluctuations we can evaluate the Fano factor F , which is essential to predict whether the shot noise lies in the Poisson or the sub-Poisson regime, through the relation [21],

$$F = \frac{S}{2eI} \quad (7)$$

For $F = 1$, the shot noise achieves the Poisson limit where no electron correlation exists between the charge carriers. On the other hand, for $F < 1$, the shot noise reaches the sub-Poisson limit and it provides the information about the electron correlation among the charge carriers.

Here, we study the transport properties at much low temperature (5 K), but the qualitative behavior of all the results are invariant up to some finite temperature (~ 300 K). For simplicity we take the unit $c = e = \hbar = 1$ in our present calculations.

3 Results and their interpretation

In this section we investigate the characteristic properties of conductance as a function of injecting electron energy, current and noise power of its fluctuations as a function of the applied bias voltage for four different polycyclic hydrocarbon molecules (Fig. 1). These molecules are defined as naphthalene (two rings), anthracene (three rings), tetracene (four rings) and pentacene (five rings), respectively. To emphasize the interference effects on the electron transport, we attach the electrodes (source and drain) to the molecules in the two distinct configurations. One is the so-called *cis* configuration, denoted by the position α - α (first column of Fig. 1)

and the other one is the so-called *trans* configuration which is defined by the notation β - β (second column of Fig. 1). Contacting the molecules to the electrodes in these two different ways we can control very nicely the interference conditions of the electronic waves traversing through different arms of the molecular rings, and, we will see that the electron transport properties are significantly affected by these interference effects. In the actual exper-

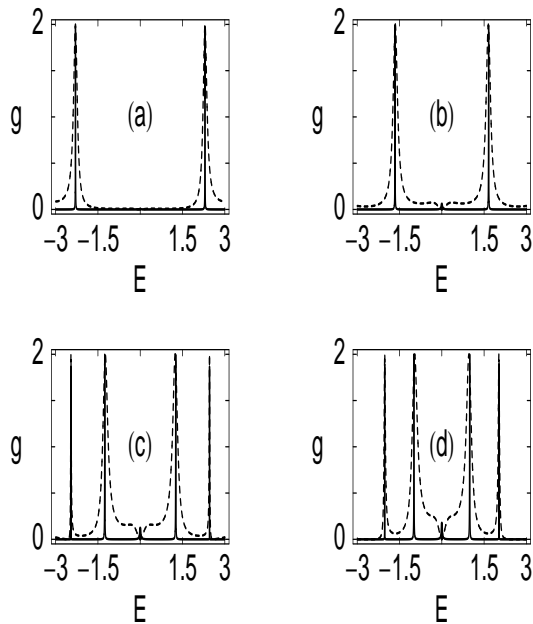


Figure 2: Conductance g as a function of the injecting electron energy E for the molecules attached to the electrodes in the *cis* configuration. (a), (b), (c) and (d) correspond to the results for the naphthalene, anthracene, tetracene and pentacene molecules, respectively. The solid and dotted curves denote the weak- and higher-coupling limits, respectively.

imental set-up, the electrodes are generally constructed from gold and the molecules are attached to the electrodes via thiol (sulfur-hydrogen i.e., S-H bond) groups in the chemisorption technique where the sulfur atoms remove and the hydrogen atoms reside.

We will study all the essential features of electron transport through the polycyclic hydrocarbon molecules in the two distinct regimes. One is the so-called weak-coupling regime defined as $\tau_{S(D)} \ll t$ and the other one is the higher-coupling regime specified as $\tau_{S(D)} \sim t$, where τ_S and τ_D are the hopping strengths of a molecule to the source and drain, respectively. In our calculations, the pa-

parameters for these two distinct regimes are chosen as: $\tau_S = \tau_D = 0.5$, $t = 3$ (weak-coupling) and $\tau_S = \tau_D = 2.5$, $t = 3$ (higher-coupling). Here we take the site energy $\epsilon_i = 0$ for all the sites of the molecules (for simplicity), and, fix the Fermi energy E_F at 0.

In Fig. 2, we plot the conductance (g) as a function of the injecting electron energy (E) for the molecules attached to the electrodes in the *cis* configuration, where (a), (b), (c) and (d) correspond to the results for the naphthalene, anthracene,

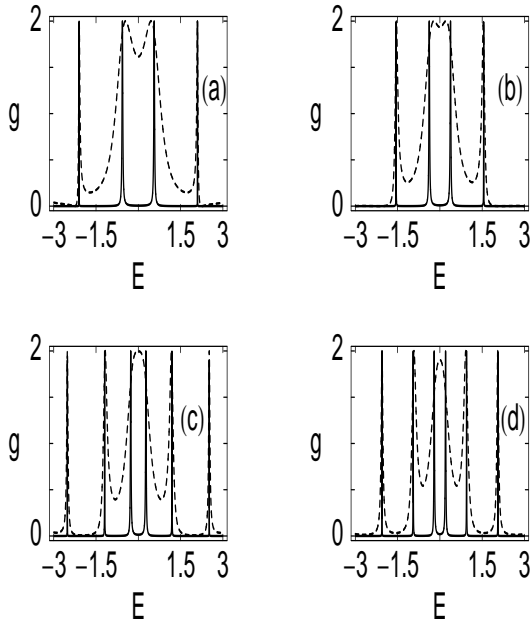


Figure 3: Conductance g as a function of the injecting electron energy E for the molecules attached to the electrodes in the *trans* configuration. (a), (b), (c) and (d) correspond to the results for the naphthalene, anthracene, tetracene and pentacene molecules, respectively. The solid and dotted curves denote the weak- and higher-coupling limits, respectively.

tetracene and pentacene molecules, respectively. The solid curves correspond to the results for the weak-coupling limit, while the dotted curves denote the results in the limit of higher molecular coupling. In the weak molecular coupling limit, the conductance shows very sharp resonant peaks (solid curves in Fig. 2) for some specific energies, while for all other energies it (g) almost drops to zero. At these resonances the conductance g achieves the value 2, and accordingly, the transmission probability T goes to unity, since from the Landauer conductance

formula we get $g = 2T$ (see Eq.(1) with $e = h = 1$ in our present calculations). These resonant peaks are associated with the energy eigenvalues of the corresponding molecule and hence more resonant peaks appear with the increment of the length of the molecule. Thus it can be emphasized that the conductance spectrum manifests itself the energy eigenvalues of the molecule. Now with the increase of the molecular coupling strength, the widths of these resonant peaks get enhanced substantially, as shown by the dotted curves in Fig. 2. This is due to the substantial broadening of the molecular energy levels in the limit of higher molecular coupling. The contribution for this broadening of the energy levels comes from the imaginary parts of the self energies Σ_S and Σ_D , respectively [40]. Therefore, for the higher-coupling limit, the electron conducts across the molecules for the wide range of energies, while a fine tuning in the energy scale is necessary to get the electron conduction through the molecules in the limit of weak molecular coupling. Hence, it can be predicted that the molecule-to-electrode coupling strength has a significant role in the determination of the electron conduction through the molecular bridges.

Figure 3 corresponds to the conductance-energy characteristics for the molecules attached to the electrodes in the *trans* configuration, where (a), (b), (c) and (d) represent the results for the naphthalene, anthracene, tetracene and pentacene molecules, respectively. The solid and dotted curves correspond to the identical meaning as in Fig. 2. Similar to the case of Fig. 2, here we also get the sharp resonant peaks in the conductance spectra for the weak-coupling limit (solid curves of Fig. 3), and, they (resonant peaks) get broadened in the limit of higher molecular coupling (dotted curves of Fig. 3). The explanations for such behaviors are the same as we discuss earlier. From this figure (Fig. 3), it is observed that both for the weak- and higher-coupling limits, more resonant peaks appear in the conductance spectra i.e., we get more resonating energy eigenstates compared to the results obtained for the *cis* configuration (Fig. 2). This feature can be explained as follows. When the molecule is attached to the electrodes, its energy eigenvalues get modified by the two self-energies Σ_S and Σ_D , respectively. The self-energies contain the real and imaginary parts, where the real part corresponds to the energy shift and the imaginary part gives the broadening of the molecular energy levels [40]. By changing the positions of the two electrodes from one configuration to the other i.e., either from the

cis to the *trans* configuration or inverse of that, the molecular energy levels are shifted in different ways, and accordingly, we get more/less resonating energy eigenstates in the scale of the energy E . This provides different resonant peaks in the conductance spectra for the two different cases (see Figs. 2 and 3). Another significant observation is that, in the higher-coupling case the probability amplitude of getting an electron across the molecular ring in the

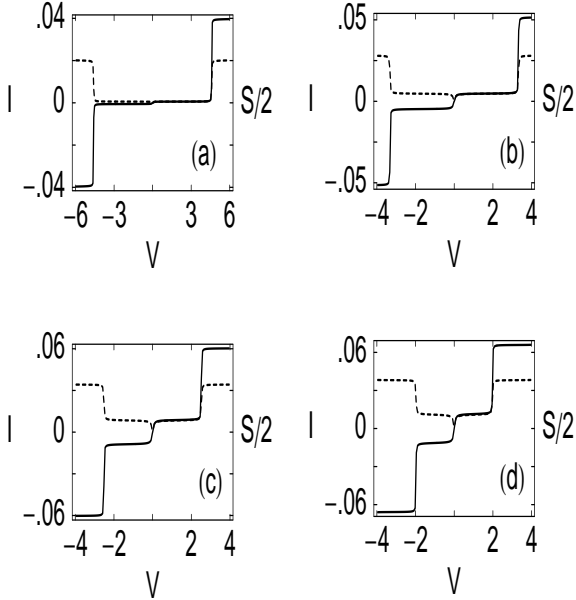


Figure 4: Current I (solid curve) and the noise power of its fluctuations S (dotted curve) as a function of the applied bias voltage V for the molecules attached to the electrodes in the *cis* configuration in the limit of weak molecular coupling. (a), (b), (c) and (d) correspond to the results for the naphthalene, anthracene, tetracene and pentacene molecules, respectively.

trans configuration is much greater than that of the *cis* configuration for most of the energy values, except at the resonant peaks where the amplitudes are same ($T = 1$) for both these two configurations. This is solely due to the quantum interference effect of the electronic waves traversing through different arms of the molecular rings. This can be explained very simply from the standard interpretation of the quantum mechanical theory. The electrons are carried from the source to drain through the molecules and the electronic waves propagating along the two arms of the molecular ring may suffer a relative phase shift between themselves. Ac-

cordingly, there might be constructive or destructive interference due to superposition of the electronic wave functions along the various pathways. Therefore, the probability amplitude of the electron across the molecule becomes either large or small. So electron transmission is strongly affected by the quantum interference and can be controlled by the molecule-electrode interface geometry. It is observed that the qualitative features of the g - E characteristics are in good agreement with the ex-

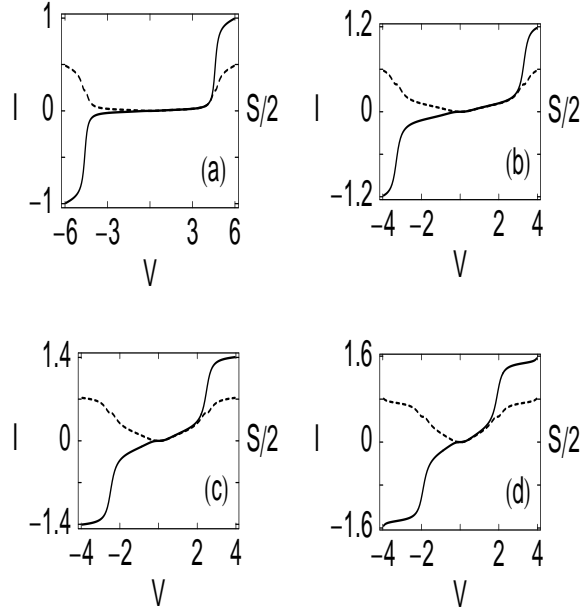


Figure 5: Current I (solid curve) and the noise power of its fluctuations S (dotted curve) as a function of the applied bias voltage V for the molecules attached to the electrodes in the *cis* configuration in the limit of higher molecular coupling. (a), (b), (c) and (d) correspond to the results for the naphthalene, anthracene, tetracene and pentacene molecules, respectively.

perimental results. Now these interference effects can be visible much more clearly by investigating the current-voltage (I - V) characteristics across the molecules and in the forthcoming parts we will describe the current and the noise power of its fluctuations as a function of the applied bias voltage for both the *cis* and the *trans* configurations.

Both the current (I) and the noise power of its fluctuations (S) are calculated from the integration procedure of the transmission function (T), as given in Eqs.(5) and (6). The behavior of the transmission function is exactly similar to that of the con-

ductance variation as shown in Figs. 2 and 3, differ only in magnitude by the factor 2 since we get $g = 2T$ from the Landauer conductance formula (Eq.(1)). In Fig. 4, we plot the current and the noise power of its fluctuations as a function of the applied bias voltage for the different molecular wires in the limit of weak-coupling where the molecules are attached to the electrodes in the *cis* configuration, where (a), (b), (c) and (d) correspond to the results for the naphthalene, anthracene, tetracene and pentacene molecules, respectively. The solid and

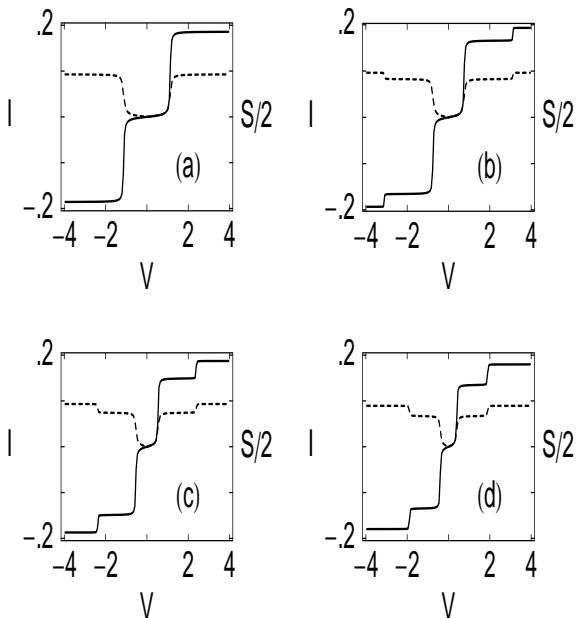


Figure 6: Current I (solid curve) and the noise power of its fluctuations S (dotted curve) as a function of the applied bias voltage V for the molecules attached to the electrodes in the *trans* configuration in the limit of weak molecular coupling. (a), (b), (c) and (d) correspond to the results for the naphthalene, anthracene, tetracene and pentacene molecules, respectively.

dotted curves denote the current and noise power, respectively. Current shows the staircase-like behavior with sharp steps as a function of the applied bias voltage. This is due to the existence of sharp resonant peaks in the conductance spectra (see the solid curves of Fig. 2), since the current is evaluated from the integration method of the transmission function T . With the increase of the applied bias voltage, the electrochemical potentials on the electrodes are shifted gradually and finally cross one of the molecular energy levels. Therefore, a current

channel is opened up and a jump in the current-voltage characteristic curve appears. More steps appear as we increase the length of the molecule associated with the molecular resonant states. For all these molecular bridges the current amplitudes are very small and they are comparable to each other (solid curves of Fig. 4). Another significant observation is that the threshold bias voltage of the electron conduction through the bridge decreases gradually with the increase of the length of the molecule. Thus, by controlling the length of the molecule we can tune the threshold bias voltage which provides a key idea for fabrication of efficient molecular switch. Now in the study of the noise power of current fluctuations for these molecular bridges in this weak-coupling limit (dotted curves of Fig. 4) we see that the shot noise goes from the Poisson limit ($F = 1$) to the sub-Poisson limit ($F < 1$) as long as we cross the first step in the current-voltage characteristics. This reveals that the electrons are correlated after the tunneling process has occurred. Here the electrons are correlated only in the sense that one electron feels the existence of the other according to the Pauli exclusion principle, since we have neglected all other electron-electron interactions in our present formalism. Another important observation is that the amplitudes of the noise power in the sub-Poisson region for all these bridges are almost invariant. These results emphasize that in the limit of weak-coupling the noise power of the current fluctuations within the sub-Poisson limit remains in the same level independent of the length of the molecule.

The characteristic properties of the current and noise power of its fluctuations are also very interesting for these molecular bridges (molecules attached to the electrodes in the *cis* configuration) in the limit of higher molecular coupling. The results are represented in Fig. 5, where (a), (b), (c) and (d) correspond to the results for the same molecular bridges as given in Fig. 4, respectively. The solid and dotted curves denote the same meaning as in Fig. 4. It is observed that the current varies quite continuously (solid curves of Fig. 5) with the applied bias voltage V . This is due to the broadening of the resonant peaks in this higher-coupling limit (see the dotted curves of Fig. 2), as the current is computed from the integration procedure of the function T . The key observation is that the current amplitudes get enhanced quite significantly compared to the current amplitudes observed for the molecular bridges in the weak-coupling limit (see the solid curves of Fig. 4). This can be em-

phasized very simply by noting the areas under the curves in the conductance spectra for these two coupling cases (Fig. 2). It is also noted here that the current amplitude increases gradually as we increase the length of the molecule for this higher-coupling limit. Now in the determination of the noise power of the current fluctuations, we see that the shot noise makes a transition from the Poisson

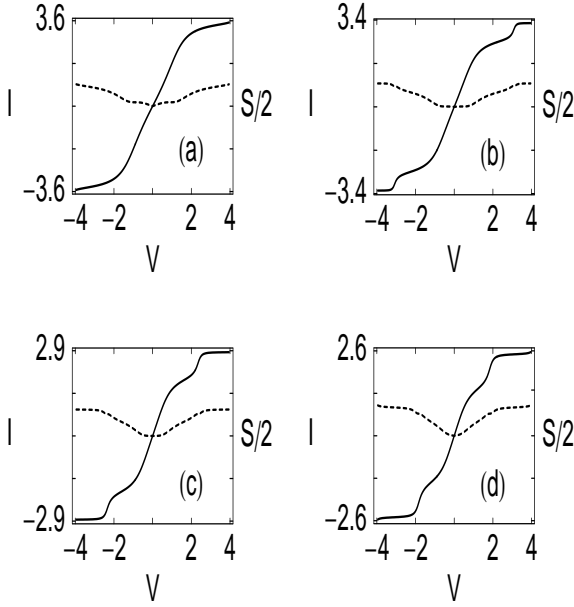


Figure 7: Current I (solid curve) and the noise power of its fluctuations S (dotted curve) as a function of the applied bias voltage V for the molecules attached to the electrodes in the *trans* configuration in the limit of higher molecular coupling. (a), (b), (c) and (d) correspond to the results for the naphthalene, anthracene, tetracene and pentacene molecules, respectively.

limit ($F = 1$) to the sub-Poisson limit ($F < 1$) after some critical value of the applied bias voltage (see the dotted curves of Fig. 5). This critical value of the bias voltage decreases gradually as we increase the length of the molecule so that the shot noise goes faster to the sub-Poisson limit for the longer molecules. Therefore, it predicts that the electron correlation is much more significant for the molecules with higher length than that of the shorter ones. In this limiting case we also see that, like as in the weak-coupling case, the amplitudes of the noise power in the sub-Poisson regime for all these bridges are almost comparable to each other.

Now focus our attention on the current and noise

power of its fluctuations for the molecules attached to the electrodes in the *trans* configuration. In Fig. 6, we plot the results for the molecules attached to the electrodes in the *trans* configuration in the limit of weak molecular coupling, where (a), (b), (c) and (d) correspond to the results for the naphthalene, anthracene, tetracene and pentacene molecules, respectively. The solid and dotted curves represent the same meaning as in Figs. 4 and 5. Like as in the *cis* configuration, for the weak-coupling limit here we also see that the current shows staircase-like behavior with sharp steps (see the solid curves of Fig. 6) as a function of the applied bias voltage and the shot noise makes a transition from the Poisson limit to the sub-Poisson limit as we cross the first step in the I - V curves (see the dotted curves of Fig. 6). The explanations of such behaviors are the same as before. The strange observation is that the current amplitudes for all these molecular wires get enhanced quite significantly, though we are in the weak-coupling limit, compared to the current amplitudes obtained for these molecules in the *cis* configuration. This is solely due to the quantum interference effects of the electronic waves traversing through the different arms of the molecular rings (Fig.1). Thus interference effects play significant role in the determination of the current through the molecular bridges. Here also, like as in Fig. 4, the noise power of the current fluctuations lies in the same level within the sub-Poisson limit (see the dotted curves of Fig. 6), independent of the length of the molecule.

Figure 7 displays the results for the molecular bridges (molecules attached to the electrodes in the *trans* configuration) in the limit of higher-coupling, where (a), (b), (c) and (d) correspond to the same molecules as in Fig. 6. The current varies continuously (solid curves of Fig. 7) with the bias voltage V for all these bridges, similar to the results studied earlier for the bridges in the *cis* configuration (solid curves of Fig. 5). For this higher-coupling limit the current amplitudes are also very large than the results obtained for the bridges in the *cis* configuration with higher molecular coupling and the explanation for such kind of behavior is the same as we describe earlier. Here it is observed that the current amplitude decreases gradually as we increase the length of the molecule, in contrary to the results predicted in Fig. 5. Our calculations of the noise power of the current fluctuations for such bridges provide that there is no such possibility of transition from the Poisson limit to the sub-Poisson limit since the shot noise already achieves the sub-

Poisson limit (see the dotted curves of Fig. 7), momentarily as we switch on the bias voltage. Accordingly, for such bridges in this limit of molecular coupling the electron correlation is highly significant. Thus we can predict that the noise power of the current fluctuations strongly depends on the molecule-to-electrode interface geometry as well as the molecule-to-electrode coupling strength.

4 Concluding remarks

In summary of this article, we have introduced parametric calculations based on the tight-binding model to investigate the electron transport properties through some polycyclic hydrocarbon molecules attached to two metallic electrodes. We have shown that the electron transport properties are significantly affected by (a) length of the molecules, (b) molecule-electrode interface geometry and (c) molecule-to-electrode coupling strength. All the results described here provide several key ideas for fabrication of efficient molecular devices.

The conductance shows fine resonant peaks for the weak-coupling limit (solid curves of Figs. 2 and 3), while they get broadened in the limit of higher molecular coupling (dotted curves of Figs. 2 and 3). This increment of the resonant widths is due to the broadening of the molecular energy levels, where the contribution comes from the imaginary parts of the self energies Σ_S and Σ_D [40].

The quantum interference effects on the electron transport have been clearly described by studying the current-voltage characteristics. Both for the *cis* and *trans* configurations, in the limit of weak molecular coupling, the current gets the staircase-like behavior with sharp steps (solid curves of Figs. 4 and 6). On the other hand, it varies quite continuously with the applied bias voltage in the limit of higher molecular coupling (solid curves of Figs. 5 and 7). The most remarkable observation is that by increasing the molecular coupling strength one can enhance the current amplitude quite significantly. We can also tune the current amplitude in a controllable way by varying the molecule-to-electrode interface geometry associated with the quantum interference effects.

In the study of the noise power of current fluctuations, we have seen that it strongly depends on the molecule-to-electrode interface geometry as well as the molecular coupling strength. In the weak-coupling case both for the *cis* and *trans* configurations, the shot noise makes a transition from the Poisson limit ($F = 1$) to the sub-Poisson limit ($F <$

1) as we cross the first step in the I - V characteristics (dotted curves of Figs. 4 and 6) which reveals that the electrons are correlated with each other after the tunneling process has occurred. Quite similarly in the higher-coupling limit for the molecular bridges in the *cis* configuration, the shot noise makes a transition from the Poisson limit to the sub-Poisson limit beyond some critical value of the applied bias voltage V (dotted curves of Fig. 5). On the other hand, for the molecules attached to the electrodes in the *trans* configuration and in the limit of higher-coupling, there is no such possibility of transition from the Poisson limit to the sub-Poisson limit as the shot noise already lies in the sub-Poisson limit momentarily as we switch on the bias voltage (dotted curves of Fig. 7), and accordingly, for such cases the electron correlation is very much significant.

Throughout our study we have used several important approximations by neglecting the effects of electron-electron interaction, all the inelastic scattering processes, Schottky effect, static Stark effect, etc. More studies are expected to take into account all these approximations for our further investigations.

References

- [1] A. Aviram and M. Ratner, Chem. Phys. Lett. **29**, 277 (1974).
- [2] R. M. Metzger *et al.*, J. Am. Chem. Soc. **119**, 10455 (1997).
- [3] C. M. Fischer, M. Burghard, S. Roth, and K. V. Klitzing, Appl. Phys. Lett. **66**, 3331 (1995).
- [4] J. Chen, M. A. Reed, A. M. Rawlett, and J. M. Tour, Science **286**, 1550 (1999).
- [5] M. A. Reed, C. Zhou, C. J. Muller, T. P. Burgin, and J. M. Tour, Science **278**, 252 (1997).
- [6] T. Dadoosh, Y. Gordin, R. Krahne, I. Khivrich, D. Mahalu, V. Frydman, J. Sperling, A. Yacoby, and I. Bar-Joseph, Nature **436**, 677 (2005).
- [7] O. Hod, R. Baer, and E. Rabani, J. Phys. Chem. B **108**, 14807 (2004).
- [8] O. Hod, R. Baer, and E. Rabani, J. Phys.: Condens. Matter **20**, 383201 (2008).
- [9] O. Hod, R. Baer, and E. Rabani, J. Am. Chem. Soc. **127**, 1648 (2005).

- [10] O. Hod, E. Rabani, and R. Baer, *Acc. Chem. Res.* **39**, 109 (2006).
- [11] P. A. Orellana, M. L. Ladron de Guevara, M. Pacheco, and A. Latge, *Phys. Rev. B* **68**, 195321 (2003).
- [12] P. A. Orellana, F. Dominguez-Adame, I. Gomez, and M. L. Ladron de Guevara, *Phys. Rev. B* **67**, 085321 (2003).
- [13] M. Magoga and C. Joachim, *Phys. Rev. B* **59**, 16011 (1999).
- [14] J.-P. Launay and C. D. Coudret, in: A. Aviram and M. A. Ratner (Eds.), *Molecular Electronics*, New York Academy of Sciences, New York (1998).
- [15] R. Baer and D. Neuhauser, *Chem. Phys.* **281**, 353 (2002).
- [16] R. Baer and D. Neuhauser, *J. Am. Chem. Soc.* **124**, 4200 (2002).
- [17] D. Walter, D. Neuhauser, and R. Baer, *Chem. Phys.* **299**, 139 (2004).
- [18] R. H. Goldsmith, M. R. Wasielewski, and M. A. Ratner, *J. Phys. Chem. B* **110**, 20258 (2006).
- [19] M. Ernzerhof, H. Bahmann, F. Goyer, M. Zhuang, and P. Rocheleau, *J. Chem. Theory Comput.* **2**, 1291 (2006).
- [20] M. Ernzerhof, M. Zhuang, and P. Rocheleau, *J. Chem. Phys.* **123**, 134704 (2005).
- [21] Y. M. Blanter and M. Büttiker, *Phys. Rep.* **336**, 1 (2000).
- [22] S. N. Yaliraki, A. E. Roitberg, C. Gonzalez, V. Mujica, and M. A. Ratner, *J. Chem. Phys.* **111**, 6997 (1999).
- [23] M. Di Ventra, S. T. Pantelides, and N. D. Lang, *Phys. Rev. Lett.* **84**, 979 (2000).
- [24] K. Tagami, L. Wang, and M. Tsukada, *Nano Lett.* **4**, 209 (2004).
- [25] Y. Xue, S. Datta, and M. A. Ratner, *J. Chem. Phys.* **115**, 4292 (2001).
- [26] J. Taylor, H. Gou, and J. Wang, *Phys. Rev. B* **63**, 245407 (2001).
- [27] P. A. Derosa and J. M. Seminario, *J. Phys. Chem. B* **105**, 471 (2001).
- [28] P. S. Damle, A. W. Ghosh, and S. Datta, *Phys. Rev. B* **64**, R201403 (2001).
- [29] (a) M. Elstner *et al.*, *Phys. Rev. B* **58**, 7260 (1998). (b) T. Frauenheim *et al.*, *J. Phys.: Condens. Matter* **14**, 3015 (2002).
- [30] (a) P. Hohenberg and W. Kohn, *Phys. Rev.* **136**, B864 (1964). (b) W. Kohn and L. J. Sham, *Phys. Rev.* **140**, A1133 (1965).
- [31] N. Sai, M. Zwolak, G. Vignale, and M. D. Ventra, *Phys. Rev. Lett.* **94**, 186810 (2005).
- [32] N. Bushong, N. Sai, and M. D. Ventra, *Nano Lett.* **5**, 2569 (2005).
- [33] M. D. Ventra and T. N. Todorov, *J. Phys.: Condens. Matter* **16**, 8025 (2004).
- [34] V. Mujica, M. Kemp, and M. A. Ratner, *J. Chem. Phys.* **101**, 6849 (1994).
- [35] V. Mujica, M. Kemp, A. E. Roitberg, and M. A. Ratner, *J. Chem. Phys.* **104**, 7296 (1996).
- [36] K. Walczak, *Cent. Eur. J. Chem.* **2**, 524 (2004).
- [37] K. Walczak, *Phys. Stat. Sol. (b)* **241**, 2555 (2004).
- [38] M. P. Samanta, W. Tian, S. Datta, J. I. Henderson, and C. P. Kubiak, *Phys. Rev. B* **53**, R7626 (1996).
- [39] M. Hjort and S. Staftröm, *Phys. Rev. B* **62**, 5245 (2000).
- [40] S. Datta, *Electronic transport in mesoscopic systems*, Cambridge University Press, Cambridge (1997).
- [41] W. Tian, S. Datta, S. Hong, R. Reifenberger, J. I. Henderson, and C. I. Kubiak, *J. Chem. Phys.* **109**, 2874 (1998).